Optics Communications 372 (2016) 118–122

Contents lists available at ScienceDirect

Optics Communications

journal homepage: www.elsevier.com/locate/optcom

# Focusing far-field nanoscale optical needles by planar nanostructured metasurfaces

Tao Liu [a,b], Tong Wang [a,b], Shuming Yang [a,b,*], Zhuangde Jiang [a,b]

[a] State Key Laboratory for Manufacturing System Engineering, Xi'an Jiaotong Univerisity, Xi'an, Shaanxi 710049, China
[b] Collaborative Innovation Center of High-End Manufacturing Equipment, Xi'an Jiaotong University, Xi'an, Shaanxi 710049, China

ARTICLE INFO

*Article history:*
Received 21 February 2016
Received in revised form
3 April 2016
Accepted 8 April 2016

*Keywords:*
Subwavelength structures
Diffraction
Polarization
Superresolution
Optimization

ABSTRACT

Far-field nanoscale optical needles are obtained using water-immersed planar nanostructured metasurfaces illuminated with a 193 nm deep ultra-violet laser. The method is based on the vectorial angular spectrum theory and an established nonlinear optimization model. For a 50 µm-diameter metasurface with a linearly polarized beam (*x*-polarized), an optical needle with $12.4\lambda_0$ length has been produced at a mid-focal distance of 14.5 µm. The transverse beam sizes are as small as 129 nm and 59.4 nm in the *x* and *y* directions, respectively. The design results are agreed well with the rigorous electromagnetic calculations using three-dimensional finite-difference time-domain (FDTD) method with a suggested 25 nm-thick aluminum coating film for the metasurface. These far-field nanoscale optical needles are potentially applied in the fields of nanolithography, nanoprinting, and nanoscopy.


## 1. Introduction

Modulation of a non-diffraction light beam or a sharp light needle has been widely studied in the last decade [1–10]. Different methods have been proposed to generate such non-diffraction light beams. These methods can be primarily classified into three groups, based on a lens-based refraction system [1–4,6,10], a mirror-based reflection system [5,8], and a microstructure-based lens-free diffraction system [7,9]. Among these methods, the use of a nanostructured metallic-film-coated plate (metasurface) is more attractive and exhibits unique advantages. Firstly, the metasurface is a single planar, lens-free, ultra-high numerical aperture (NA) focusing element, in contrast to a bulky lens-based optical system with pupil filters [2,6,10,11]. Secondly, it obtains far-field optical sub-diffraction and super-resolution without near-field evanescent waves [12], which essentially differs from the superlens [13] or the plasmonic lens [14]. In addition, compared with a high-NA Fresnel zone plate [7], the minimum annulus width of a nanostructured metasurface is not necessarily at sub-wavelength [11,15–17], which facilitates the practical fabrication. The mechanism of a series of non-rotationally symmetrical metasurfaces was exploited and novel features were found in [18–20].

So far, although the transverse beam size of optical needles has been constantly decreased [1–11], all the methods above have not yet provided a practical approach for modulating a nanoscale optical needle with the lateral beam width close to 100 nm (or sub-100 nm) in the optical far-field region. For the traditional lens-based optical systems, the glass materials are scarce for deep ultra-violet (DUV) or extreme ultra-violet (EUV) wavelengths. The use of a cylindrical vector beam (e.g. radially polarized beam) needs a precision apparatus to produce the required amplitude distribution [2–4,11,15]. The use of the parabolic mirror or a high-NA Fresnel zone plate requires rigorous and costly fabrication techniques [5,7]. All these can be solved using a planar multi-annular nanostructured metasurface illuminated with a DUV (or EUV) light source. These metasurfaces are easy-to-fabricated using focused ion beam (FIB) or electron beam lithography (EBL) processing techniques [11,12,16]. The far-field nanoscale optical needles can be potentially used in the fields of nanolithography, nanoprinting, and nanoscopy.

## 2. Design theory and result

### 2.1. Design theory

The developed vectorial design method is based on the vectorial angular spectrum (VAS) theory and optimized using the purposely configured genetic algorithm (GA) [15,16]. This approach generalizes the scalar angular spectrum method [12] and

* Corresponding author at: State Key Laboratory for Manufacturing System Engineering, Xi'an Jiaotong Univerisity, Xi'an, Shaanxi 710049, China.
*E-mail address:* shuming.yang@xjtu.edu.cn (S. Yang).

http://dx.doi.org/10.1016/j.optcom.2016.04.022
0030-4018/© 2016 Published by Elsevier B.V.

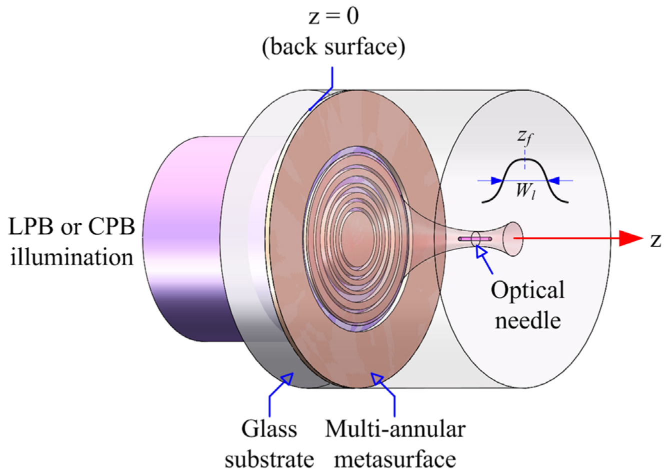


**Fig. 1.** Schematic diagram of focusing an ultra-thin optical needle by a planar multi-annular metasurface illuminated with a LPB or a CPB.

uses a fast Hankel transform algorithm to accelerate the optimization process [16]. It differs from the method based on the vectorial Rayleigh-Sommerfeld diffraction integral and binary particle swarm optimization algorithm [9,11,12]. The metasurface is composed of many concentric rings either opaque or transparent and the amplitude distribution of the incident vector beam is assumed to be rotationally symmetric. The schematic diagram of the focusing geometry is shown in Fig. 1, with a linearly polarized beam (LPB) or a circularly polarized beam (CPB). A metasurface is realized by coating a thin metallic film on a glass substrate.

According to the VAS theory, the electric field distribution behind the metasurface can be described by a specific integral representation for a linearly, circularly, or radially polarized vector beam [15–17]. For example, when a linearly polarized beam (LPB, x-polarized) normally illuminates the metasurface mask, Cartesian components of the electric field $\boldsymbol{E}$ for any point $P(r, \varphi, z)$ in the observation plane ($z > 0$) are described as

$$\begin{bmatrix} E_x(r, z) \\ E_y(r, z) \\ E_z(r, \varphi, z) \end{bmatrix} = \int_0^\infty \begin{bmatrix} J_0(2\pi lr) \\ 0 \\ -\mathrm{j}\cos\varphi \dfrac{l}{q(l)} J_1(2\pi lr) \end{bmatrix} A_0(l)\exp[\mathrm{j}2\pi q(l)z]2\pi l dl, \quad (1)$$

where $q(l) = (1/\lambda^2 - l^2)^{1/2}$ and $l$ is the transverse spatial frequency component. The light wavelength in the immersion medium is $\lambda = \lambda_0/\mu$ ($\lambda_0$ the vacuum wavelength and $\mu$ the refractive index of the immersion medium). $J_0$ and $J_1$ are the zero and first order Bessel functions of the first kind, respectively. In Eq. (1), $A_0(l) = \int_0^\infty t(r) J_0(2\pi lr) 2\pi r dr$ with $t(r)$ denoting the transmission function for the metasurface mask. The total electric energy density (or light intensity) is calculated by $I_{vas}(r, \varphi, z) = |\boldsymbol{E}(r, \varphi, z)|^2 = |E_x(r, z)|^2 + |E_z(r, \varphi, z)|^2$. If illuminating metasurfaces with a circularly polarized beam (CPB), the total electric energy density can be obtained from two orthogonally polarized linearly polarized beams, as [17]

$$I_{vas}(r, z) = 2|E_x(r, z)|^2 + |E_z(r, \varphi = 0, z)|^2, \quad (2)$$

where $E_x$ and $E_z$ are described in Eq. (1). The intensity distribution is circularly symmetric and the light beam generally becomes broader than that illuminated with a LPB.

Metasurfaces can be optimized with the required optimization targets using the 3D intensity distribution $I_{vas}$. It is elected to constrain $I_{vas}$ along two orthogonal directions, including the optical axis and a transverse axis in the mid-focus plane. Along the optical axis, a flat-top super-Gaussian function is used to simulate an optical needle [11,21]. The transverse beam size is restricted by predefining an equivalent numerical aperture ($NA_{eq}$) for the mid-focus plane via $NA_{eq} = \eta \sin\{[\tan^{-1}[D/(2z_f)]\}$. $D$ is the metasurface diameter and $z_f$ is the axial position for the mid-focus plane. Additionally, the metasurface is assumed to be central-obstructed, and the central obstruction area is also optimized. The initial metasurface structure is assumed to be composed of many concentric annuli with an equal annulus width $\Delta r$ [12]. As a result, a single-objective, multi-variable, constrained nonlinear optimization model is established as

$$\text{Minimize RMSE} = \left[\frac{\sum (I_{cal} - I_{obj})^2}{\sum I_{obj}^2}\right]^{1/2}$$

Subject to:

$$\begin{aligned} & I_{cal} = I_{vas}(0, \boldsymbol{Z}; \boldsymbol{T}) \\ & I_{obj} = K\exp[-(\boldsymbol{Z}^{2N_{sg}}/b^{2N_{sg}}) \\ & \boldsymbol{T} = \{t_i\}, \quad \boldsymbol{Z} = \{z_n\} \\ & |z_n - z_f| \le W_l/2 \\ & \varepsilon_{min} \le \varepsilon \le \varepsilon_{max} \end{aligned} \quad (3)$$

where $b = W_l/[2(\ln 2)^{1/(2N_{sg})}]$, $K = I_{vas}(0, z_f)$, and $t_i \in \{0, 1\}$, $i = 1, 2, \ldots, N$. $t_i$ is the transmission of the $i$-th annulus contained in the metasurface (0 opaque or 1 transparent) . $N_{sg}$ denotes the order of a super-Gaussian function. $N_{sg}$ is an integer, selected from {2, 3, 4, 5} in the current optimization. The sampled axial positions locate at $z_n = z_f \pm n\Delta z$, $n = 0, 1, 2, \ldots, N_{zp}/2$. The total number of evaluated positions along the axial direction is $(N_{zp}+1)$. $\Delta z$ is the axial displacement. $W_l$ is the required size of the optical needle along the axial direction and it is evaluated using the full width at half maximum (FWHM). $\Delta z$ is given as $W_l/(N_{zp} + 1)$. The central obstruction factor $\varepsilon$ is defined as the ratio of the first transparent annulus number to the total annulus number $N$. $\varepsilon$ is optimized between $\varepsilon_{min}$ and $\varepsilon_{max}$. In the following examples, $\varepsilon_{min} = 0.1$ and $\varepsilon_{max} = 0.7$. $I_{obj}$ is a super-Gaussian function. The root mean square error (RMSE) is used as the objective function. The genetic algorithm and a fast Hankel transform algorithm can be programmed to solve the above nonlinear optimization problem [15,16].

### 2.2. Simulation results

The 193 nm immersion lithography has become the key technique for the sub-100nm nanolithography with the ArF excimer laser [22]. Here, water immersed ($\eta = 1.44$) nanostructured metasurfaces are designed for this DUV wavelength ( $\lambda_0 = 193$ nm). Typical samples $M_{1\sim4}$ are designed and summarized in Table 1. The annulus width is $\Delta r = 200$ nm. $M_1$ and $M_2$ are designed for modulating far-field optical needles. $M_3$ and $M_4$ are prepared for rigorous electromagnetic validation in Section 3. $M_2$ and $M_3$ are designed with a CPB, while $M_1$ and $M_4$ are designed with an x-polarized LPB. It should be noted that a much larger metasurface can be optimized using the above method. However, the optimization process would be time-consuming and requires large computation storage.

The diameter of $M_1$ is 50 μm and it is composed of 9 transparent rings. An x-polarized LPB is used as the illumination light source. The mid-focus plane locates at $z_f = 14.5$ μm and the corresponding $NA_{eq} = 1.25$ for this transverse plane. According to the VAS theory, the light intensity distributions behind $M_1$ are plotted in Fig. 2. Fig. 2(a) and (b) show the intensity distributions ($|\boldsymbol{E}|^2$) in the $x$–$z$ and $y$–$z$ planes, respectively. In the mid-focus plane, FWHM is as sharp as 59.4 nm in the $y$ direction and it is 129 nm in the $x$ direction, as shown in Fig. 2(c). The axial intensity distribution is plotted in Fig. 2(d) and the axial width of the optical needle is $12.4\lambda_0$. The widening of the light beam in the x–z plane is due to